

OPTIMIZATION OF THICKNESS FOR SOLID ROCKET MOTOR CASING

Dr. K. Kalyani Radha, Associate Professor

JNTUACEA, Ananthapuramu, Andhra Pradesh, India.

*Corresponding Author Email: radha.mech@jntua.ac.in

Abstract: This project work is to optimize the thickness of the solid rocket motor casing, to ascertain the design margins and health of the rocket motor case. The testing procedure, instrumentation of this solid rocket motor is very difficult because of failures in sensors (strain gauges). The reasons for sensors failure:

a) Bulkiness of the tail gauges can drastically affect the aerodynamic behavior of the motor or compressor, affecting the stress / temperature distribution and vibration mode. This seriously hampers the accuracy and meaningfulness of the measurements.

b) Conventional bonding techniques cannot ensure the integrity of bond under high temperatures and centrifugal loads.

c) Reduce the thickness of rocket motor case from 6.75 mm to 4.2 mm to decrease the weight of the motor case.

Under this aggressive environment thin-film sensors applied to the blade offer practicability and functional advantage due to their low mass, superior adhesion characteristics and vastly mitigated tendency to affect the aerodynamic flows. Here developing thin-film sensor for application on hot end gas motor components such as rotor blades and nozzle guide vanes of solid rocket motor. Thin film strain sensors facilitate non-intrusive assessment of strain data from hot end components that in turn facilitates performance evaluation and service life prediction of these components.

Keywords: solid rocket motor casing, conventional bonding techniques, thin-film sensor, strain gauges.

1. INTRODUCTION

A solid rocket or a solid-fuel rocket is a rocket with a motor that uses solid propellants. A typical solid rocket motor is shown in (figure 1.1). In solid propellants both the fuel and the oxidizer are in the solid form. Solid rockets are still used today in model rockets and on larger applications for their simplicity, reliability and can remain in storage for long periods though Liquid rockets and Hybrid rockets offered more efficient and controllable alternatives. The lower performance of solid propellants (as compared to liquids) does not favor their use as primary propulsion in modern medium-to-large launch vehicles. Customarily used to orbit commercial satellites and launch major space probes. Solids are, however, frequently used as strap-on boosters to increase payload capacity or as spin-stabilized add-on upper stages when higher-than-normal velocities are required.

Load conditions. A solid propellant rocket is formed by four main components;

1. A case containing the solid propellant and withstanding internal pressure when the rocket is operating.
2. The solid propellant charge (or grain), which is usually bonded to the inner wall of the case, and occupies before ignition the greater part of its volume. When burning, the solid propellant is transformed into hot combustion products. The volume occupied by the combustion products is called combustion chamber.
3. The igniter, which can be a pyrotechnic device or a small rocket, starts the rocket operating when an electrical signal is received.
4. The nozzle channels the discharge of the combustion products and because of its shape accelerates them to supersonic velocity.

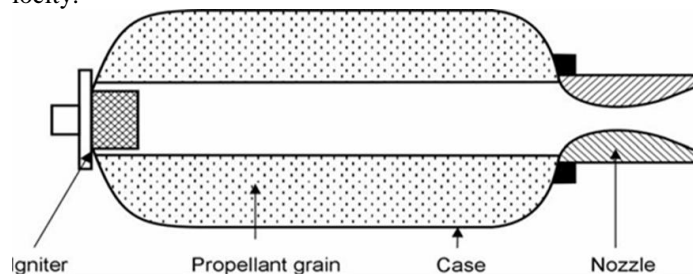


Fig-1: Typical Solid Rocket Motors

A solid-fuel rocket or solid rocket is a rocket with a rocket engine that uses solid propellants (fuel/oxidizer). The earliest rockets were solid-fuel rockets powered by gunpowder they were used in warfare by the Chinese, Indians, Mongols and Arabs, as early as the 13th century.

All rockets used some form of solid or powdered propellant up until the 20th century, when liquid-propellant rockets offered more efficient and controllable alternatives. Solid rockets are still used today in model rockets and on larger applications for their simplicity and reliability.

Since solid-fuel rockets can remain in storage for long periods, and then reliably launch on short notice, they have been frequently used in military applications such as missiles. The lower performance of solid propellants (as compared to liquids) does not favor their use as primary propulsion in modern medium-to-large launch vehicles customarily used to orbit commercial satellites and launch major space probes. Solids are,



however, frequently used as strap-on boosters to increase payload capacity or as spin-stabilized add-on upper stages when higher-than-normal velocities are required. Solid rockets are used as light launch vehicles for low Earth orbit (LEO) payloads under 2 tons or escape payloads up to 500 kilograms.

II. SCOPE AND OBJECTIVE

The scope of this project work is to optimization of the thickness of solid rocket motor case, which is a simple pressure vessel and carries out proof pressure test to ascertain the design margins and health of the rocket motor case. The testing procedure, instrumentation part, extracting results, stress calculations are discussed in detail in various chapters.

1. Design a rocket motor case, which is a pressure vessel.
2. Sensor Fabrication involves the following steps:
 - a. Study of sputter deposition processes for deposition of bond coat and insulation.
 - b. Preparation of masks
 - c. Sputter coating and testing of the coated thin film layers.
 - d. Study the variation of the resistivity of nichrome film up to 2000K
 - e. Characterization of the test coupons to evaluate insulation resistance, grid resistance, allowable strain, strain-resistance linearity, gauge factor.
- F. Optimization of sputter deposition parameters
- G. Deposition of thin film strain sensors as defined on industrial components
3. Studies on sensor endurance under harsh environments and accuracy of sensor data.
4. Finalizing instrumentation plan and testing procedure for proof pressure test.
5. Carry out test as per procedure.
6. Calculation of stress from strains.
7. Determining margin of safety on the motor case and the acceptance of the casing.

III. THICKNESS REDUCTION

Reduce the weight of the solid rocket motor by decreasing the thickness of the solid rocket motor casing. This gives a lesser

weight Rocket. If we reduce weight of one solid rocket motor case may give 5% weight decrement in total weight of the Rocket. If we reduce the wall thickness of solid rocket motor case, there are two more problems will rise. Those problems are:

a. Hoop stress (internal pressure) increases inside of the solid rocket motor casing. This leads to burst out the casing.

Increase the time and cost of the instrumentation because of sensor failures. To overcome the first problem, we use proper materials based on their extensive properties. And to overcome the second problem by using the developed multilayer thin film sensors while testing of the solid rocket motor casing.

c. Material selection:

There are three types of materials used for design the solid rocket motor casing. Those materials are listed in the table.

PROPERTY	MATERIAL1 15CDV6	MATERIAL2 M250	MATERIAL3 TITANIUM ALLOY
UTS	980MPa	1800MPa	2100MPa
% OF ELONGATION	10	15	6
YIELD STRENGTH	835MPa	1500MPa	1800MPa
YOUNG'S MODULOUS	210GPa	210GPa	210GPa
POISSON'S RATIO	0.3	0.2	0.15

Table: properties of different materials used for rocket casing

The design inputs are given below

Pressure (P)	=	5.4MPa
Diameter (D)	=	1000mm
Mismatch Factor	=	1.15
Biaxial gain	=	10%



Factor of safety	=	1.125 of Y.S
Weld efficiency	=	90%
Weld mismatch in L-seam (d)	=	5% (max)
Weld mismatch in C-seam	=	10% (max)
Biaxial gain	=	10%

Formulas used:

$$\bullet \text{ Allowable stress (S.E)} = \frac{\text{yield strength} * 0.9}{f_{os}}$$

$$\bullet \text{ Thickness (t)} = \frac{p * d * \text{mismatch factor}}{(1 + \text{biaxial gain}) * 2 * (SE - 0.6 * p)}$$

Material 15cdv6 (low carbon stainless steel forged plate):

$$\text{S.E (allowable stress)} = \frac{835 * 0.9}{1.125} = 668 \text{MPa}$$

$$\text{Wall thickness of the S.R.M.C} = \frac{5.4 * 1000 * 1.15}{(1 + 0.1) * 2 * (668 - (0.6 * 5.4))} = 4.246 \text{mm}$$

Head end and nozzle end dome thickness (ellipsoidal dome):

Pressure	=	5.4Mpa
Major axis (a)	=	500 mm
Minor axis (b)	=	300 mm
Allowable stress (S.E)	=	668Mpa
Weld mismatch (k1)	=	1.15
Opening factor (K2)	=	1.10

Formulas used:

$$\text{Thickness (t)} = \frac{(p * a^2 * k1 * k2)}{2 * d * S.E}$$

$$= \frac{5.4 * 500^2 * 1.1 * 1.15}{2 * 300 * 668} = 4.232 \text{ mm.}$$

Material M250 (maraging alloy steel):

$$\text{S.E (allowable Stress)} = 1200 \text{Mpa}$$

$$\text{Wall thickness of the S.R.M.C} = 2.35 \text{ mm}$$

$$\text{Ellipsoidal dome thickness} = 2.371 \text{ mm}$$

Material titanium alloy steel:

$$\text{S.E (allowable Stress)} = 1440 \text{Mpa}$$

$$\text{Wall thickness of the S.R.M.C} = 1.96 \text{ mm}$$

$$\text{Ellipsoidal dome thickness} = 1.97 \text{ mm}$$

As per the inputs taken by the teardown and benchmarking technics, we calculated the allowable stresses and corresponding wall thicknesses of solid rocket motor casing. 15cdv6 material having more thickness with compare to other two materials. If we use M250, Titanium alloy steels we get very less weighted rocket motor casing. But manufacturing and their structural characteristics with increasing the temperature inside solid rocket motor casing was not good with compared to 15cdv6.

M250 (maraging alloy steel) having more strength with compared to 15cdv6 and it can withstand up to 2.3 mm thickness. But it is not having constant structure with increasing the temperature. It changes the body structure according to the temperature increment. And also it is not having good % of elongation so this material will not suitable for manufacturing of solid rocket motor casing with our design inputs.

Titanium alloy steel having more strength with compared to 15cdv6 and M250 and it can withstand up to 1.96 mm thickness. But it is having oxides in atomic structure. Those oxides may lead to corrosion inside wall of the solid rocket motor; this generates an adverse effect of increasing surface roughness. More surface roughness will create improper burning of solid propellant. Weld ability of this material also very difficult and we have to use more accurate machines to perform welding in manufacturing of solid rocket motor case. This material is more cost with compared to other two materials and availability of this material also very less, so we have to import that material from other countries. After discussing all parameters we selected 15cdv6 is the suitable material to manufacture the solid rocket motor case with wall thickness of 4.2 mm.

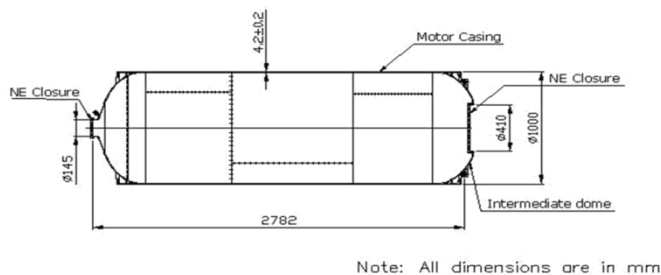


Fig2: Rocket motor designed with calculated thickness

IV. FABRICATION OF MULTILAYER THIN FILM SENSORS

Hot section components of aero gas turbine engines including turbine rotor discs, blades, nozzle guide vanes etc. operate at high temperature in excess of 1000°C. Assessment of temperature and strain data from these components is indispensable for determining the performance, engine health and life consumption. Conventional foil Strain gauges is one of the most widely used in experimental stress analysis. Strain gauges are used for measuring both static & Dynamic Strain and the strain data is captured through dedicated instrumentation that sometimes can include slip ring and telemetry system. Conventional foil gauges that are housed on polyamide carriers can be bonded to only cool section components like fan rotors and stators. These gauges are attached to the component surfaces using techniques like soldering / spot welding / bonding / cementing using cyanoacrylate adhesives. These foil gauges have thickness of ~ 50 μm and they remain thermally stable up to about 200°C. For high temperature applications thin film sensors are preferred over foil sensors because thin films (~ 50 μm) cause relatively low distortion to aerodynamic gas flows and more significantly remain stable upto about 1100°C.

Conventional foil gauges are not suitable for high temperature applications due to:

- Bulkiness of the foil gauges can drastically affect the aerodynamic behavior of the turbine or compressor, affecting the stress / temperature distribution and vibration mode. This seriously hampers the accuracy and meaningfulness of the measurements.
- Conventional bonding techniques can't ensure the integrity of bond under high temperatures and humongous centrifugal loads. (>20000g).

Under this aggressive environment thin-film sensors applied to the blade offer practicability and functional advantage due to their low mass, superior adhesion characteristics and vastly mitigated tendency to affect the aerodynamic flows.

Here developing thin-film sensor for application on hot end gas turbine components such as turbine rotor blades and nozzle guide vanes of aero gas turbine engines. Thin film strain sensors facilitate non-intrusive assessment of strain data from hot end components that in turn facilitates performance evaluation and service life prediction of these components.

Steps in Fabrication of thin film sensors:

- Preparation of test coupons out of Nickel based super alloys
- Sputter deposition of thin film strain sensors with following architecture
 - Metallic bond coat (Three options of metallic bond coat viz., FeCrAlY, CoCrAlY or NiCoCrAlY 50 μm)
 - Al_2O_3 insulation layer (6 μm)
 - Ni Cr sensor film (1 μm)
 - Protective Al_2O_3 layer (1 μm)
- Extensive characterization of thin film sensor
 - For the bond coat
 - Thickness
 - Elemental analysis,
 - Stoichiometry analysis
 - Electrical properties
 - Residual film stress if any.
 - For Al_2O_3 layer,
 - Thickness,
 - Insulation resistance,
 - Structure/microstructure analysis
 - Electrical properties
 - For the NiCr Layer (Sensor layer)
 - Thickness
 - Elemental analysis,
 - Structure/microstructure analysis
 - Gauge resistance
 - Thermal stability and

- Gauge factor (sensor calibration)
- Sensor coated on flat substrates would be subjected thermal cycling (upto 1200K) to verify:
 - Thermal stability
 - Variation in resistance as a function of temperature

(d) Deposition Trials on Industrial Components

Experimental Materials and Method:

The most important planned application for the thin film sensors is in the hot section of the gas turbine Engine. Both high pressure Motor blades and nozzle guide vanes have significant needs for accurate surface temperature measurements in commercial and gas turbine engines. Discussions with DRDO engineers were used to select the IN718 materials as the high pressure turbine blade and nozzle guide vanes. Subsequent negotiations to obtain the materials from the manufacturers favored the IN718. The standard coating techniques sputtered Processes. Sputtering targets MCrAlY and Alumina (Al_2O_3), NiCr procured from AJA International. This approach has several advantages: it ensures that the material systems represent the state of the art advanced turbine engine material technology and it simplifies the transfer of gained technology to commercial practice.

Test Coupon Design:

The test coupon, design for this investigation is intended to simulate the applications of thin film sensors on present and near future turbine Engine first stage turbine blades and vanes. A schematic cross section of the thin film sensor is presented in Figure 5.1 with the thickness of each layer of the device.

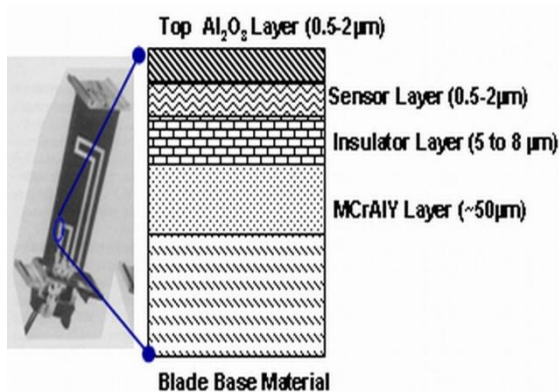


Fig3: Architecture of Thin Film Sensors

These thickness relationships must be preserved in the test coupon design to preserve the thin film sensor and simulate the stress and strain environment of the actual application. All the test coupons used in the investigation were prepared and coated by commercial processes to insure direct correspondences of metallurgical structural aspects. The test coupon design also had the following requirements. It must be suitable for thermal oxidation; surface grinding, polishing, and cleaning; sputtering of uniform layers; electrical performance evaluation up to 1100°C. To efficiently and economically satisfy the above requirements, a flat test coupon approximately 2mm x 2 mm x 62micrometers was employed which was suitable for all requirements. A metal masking technique was chosen for obtaining the sensor pattern. Steel shim stock 0.12 mm thick was chosen as the masking material and it could be cut approximately 0.3 mm tolerances.

SURFACE PREPARATION:

To ensure good adhesion of the layers to the substrate and also to mitigate the layer inhomogeneity's that can affect the insulation, surface of the substrate should be prepared to an excellent finish ($R_a \sim 0.8\mu m$). Since electrolytic polishing induces inhomogeneous surface state and high roughness and some other processes such as burnishing, grinding, micro peening, dry and wet blasting.

Standardization of the Sputtering Parameters: Sputtering is one of the most versatile techniques used for the deposition of thin films when device quality films are required. Sputtering process produces films with higher purity and better controlled composition, provides films with greater adhesion and homogeneity and permits better control of film thickness. The sputtering process involves the creation of gas plasma usually of an inert gas such as argon by applying voltage between a cathode and anode. The cathode is used as a target holder and the anode is used as a substrate holder. Source material is subjected to intense bombardment by ions. By momentum transfer, particles are ejected from the surface of the cathode and they diffuse away from it, depositing a thin film onto a substrate. Sputtering is normally performed at a pressure of $10^{-2} - 10^{-3}$ Torr.

There are two modes of powering the sputtering system; dc and RF biasing. In dc sputtering system a direct voltage is applied between the cathode and the anode. This method is restricted for conducting targets only. RF sputtering is suitable for both conducting and non-conducting targets; a high frequency generator (13.56 MHz) is connected between the electrodes of the system.

In the process of sputtering, the material is knocked out of a surface by heavy argon ions and travel across the system to condense onto the substrate surface. For the sputtered material to arrive at the substrate surface with the high energy necessary to give a good coating, and for the process to be efficient, it is important for the material to travel without collision with the residual gas in the vacuum. However, the residual gas pressure needed to maintain a simple electrical discharge, in order to provide the argon ions for bombardment, is too high to allow transfer of the sputtered material without many collisions. This gives rise to a very slow deposition rate and poor quality coating. A magnetron uses a magnetic field to confine electrons close to the cathode, making it easier to sustain an electrical discharge at low pressure. Magnetron sputtering is particularly useful when high deposition rates and low substrate temperatures are required. Both reactive and non-reactive forms of dc, RF and magnetron sputtering have been employed for the deposition of semiconducting transparent thin films. In reactive sputtering, the reactive gas is introduced into the sputtering chamber along with argon to deposit oxide films. The deposition rates and properties of the films strongly depend on the sputtering conditions such as the partial pressure of the reactive gas, the sputtering pressure, substrate temperature and target to substrate spacing.

The atom diffuses around the substrate with a motion determined by its binding energy to the substrate, which is influenced by the nature and temperature of the substrate. The depressions on the substrate surface act as adsorption sites for the diffusing atoms. At each hop, the atom will either jump over the barrier into an adjacent site or will re-evaporate. After a certain time, the atom will either evaporate from the surface or will join another diffusing single atom to form a doublet. These doublets will be joined by other single atoms to form triplets, quadruplets and so on. This stage is known as the nucleation stage of thin film growth and it leads to the formation of quasi-stable islands. The islands will grow in size and it will lead to the coalescent stage. Coalescence proceeds until the film reaches continuity.

Sputtering may be carried out in a variety of systems, which may differ in sputtering configuration, geometry, target type etc. Experimental sputtering systems usually have small targets and low production rates, whereas commercial production systems have large targets and rapid substrate transport to maximize production rate. Irrespective of the sputtering system used, the basic sputtering process remains the same. Figure 3.1 shows a typical sputter deposition system.

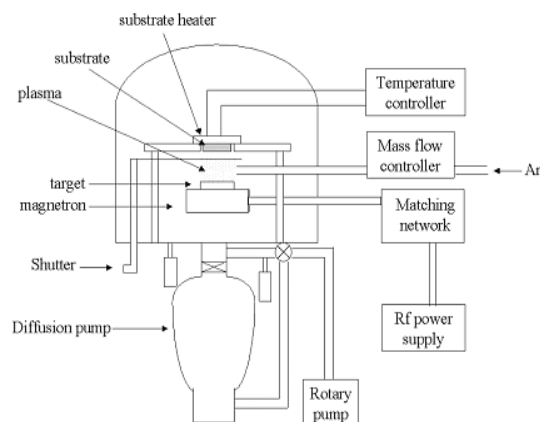


Fig5: Schematic sketch of RF sputter deposition system

The films are deposited by RF/DC Magnetron Sputtering System with targets 4'' diameter & targets 2'' diameter. A single sputtering system (ARC16M-2GRTD, TORR International New Windsor, NY, Figure 3.2) was used to obtain the consecutive layers. Studies on the sputtering parameters were conducted so as to optimize the deposition.



Fig4: Sputtering system used for deposition of the films

The standardization of the sputtering parameters (sputtering power and pressure) is important because once, we have the optimum growth condition of the thin films then we can deposit the thin films of given thickness by controlling the deposition time.

Design & Development of Mask Pattern for Sensor Layer

Specification of Mask Pattern for Sensor Layer

Dimensions:

$l=14\text{mm}$
 $l_g=8\text{mm}$
 $w=80\ \mu\text{m}$

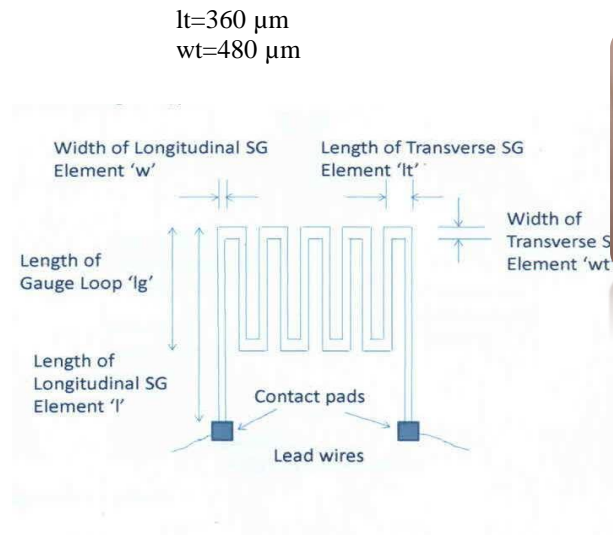


Fig6: Sensor pattern

Design of Sensor pattern or mask

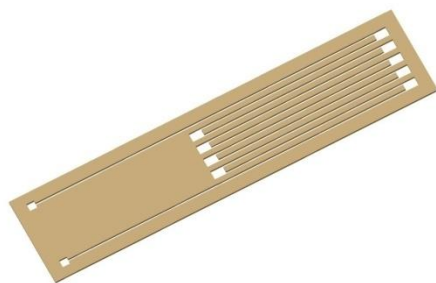


Fig7: Pattern Design for Sensors Layer

Fabrication of Sensor Pattern or Mask:

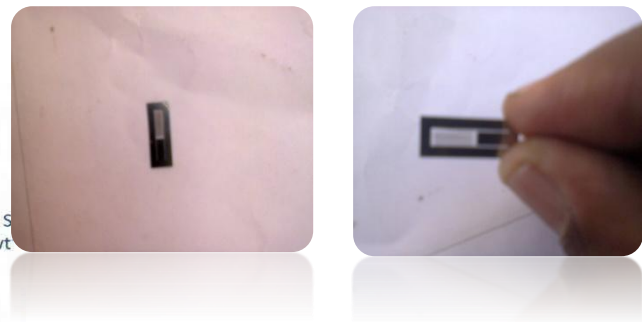


Fig8: Sensor Pattern

Strain gauge specifications:

- Gauge factor: 2.5
- Strain Range: $1000\mu\epsilon$
- Apparent Strain sensitivity: $116\mu\epsilon/\text{oC}$
- Loads: 120kg
- Rotating speed: 18000RPM
- Temperature coefficient of resistance: 290 ppm/oC
- Operating temperature: 700oC
- Low Cycle Fatigue: 3500 cycles at operational conditions (18000RPM + 550oC)
- High Cycle Fatigue: $\pm 2000\mu\epsilon$ at 1million cycles.

Developing the sensor on IN718 coupons:

- Choosing suitable strain gauge material
- Fabrication of strain gauge device on IN718 coupons
- Lead out track (Taking contact from strain gauge device to electronic circuit).
- Characterization of strain gauge device under simulated condition.

Layers	Chosen Material
Bond Coat Layer	MCrAlY
Insulation Layer	Al ₂ O ₃
Sensor layer	NiCr



Protecting layer

A1203

V. TESTING

Proof pressure test is a type of acceptance test carried out on all the components, to establish the design margins and to prove the quality of manufacturing process involved in fabrication of components. This chapter deals with the assembly procedure, testing methodology and test results.

Fig9:Strain gauge locations in the solid rocket motor

Testing Procedure:

I. Make all the sensors readings to zero before start of the test.
 ii. Increase pressure to 1.0 MPa and check for leak at all the interfaces.

iii. Rectify leak if any otherwise go ahead with the test.

iv. Do a cyclic test as per the cycle and check all the readings of all the sensors for its functionality.

0 - 0.3 - 1.0 - 2.0 - 0.5 - 0 (Pressure in MPa)

v. Carry out the test as per the cycle given

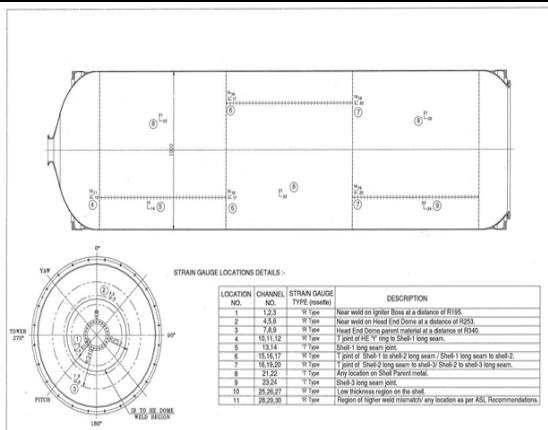
0 - 1.0 - 2.0 - 3.0 - 4.0 - 5.0 - 5.4 - 5.6 - (hold 3min) - 5.4 - 5.0 - 4.0 - 3.0 - 2.0 - 1.0 - 0 (Pressure in MPa)

vi. Hold for 10 seconds at each pressure level for the pressure to stabilize and record the readings.

vii. Remove oil and disassemble the closures.

viii. Check for any abnormality in bolts and gaskets after test.

	Pressure(Mpa)								
	1			3			5.4		
	STRAIN(μstrain)			STRAIN(μstrain)			STRAIN(μstrain)		
	€1	€2	€3	€1	€2	€3	€1	€2	€3
	0°	45°	90°	0°	45°	90°	0°	45°	90°
1	639	560	471	1827	1580	1304	3278	2759	2172
2	363	332	272	1060	966	794	2005	1819	1413
3	29	161	307	83	477	907	160	877	1652
4	444	315	265	1254	948	795	2283	1811	1520
5	918	596	223	2434	1566	589	4755	2927	1051
6	243	240	158	1113	918	512	2321	1816	917
7	316	160	57	1251	671	207	2703	1536	534
8	575	407	214	1688	1164	537	3266	2191	908
9	650	451	247	1965	1313	613	3790	2475	1042



Test Photo



Calculations:

From the input values tabulated above, the principal stresses (σ_1, σ_2) corresponding to principal strain values (ϵ_p, ϵ_q) and Vonmises stresses (σ_v) for a given pressure value are calculated as follows at location 1.

Calculations are done with $E = 210\text{GPa}$, $\nu = 0.3$ and strains as micro strains

For a given pressure value of 2MPa, we have $\epsilon_1 = 1247$, $\epsilon_2 = 1085$, $\epsilon_3 = 902$

Formula used:

$$\epsilon_p, q = \frac{\epsilon_1 + \epsilon_3}{2} \pm \frac{1}{\sqrt{2}} * \sqrt{(\epsilon_1 + \epsilon_2)^2 + (\epsilon_2 - \epsilon_3)^2}$$

$$\sigma_1 = \frac{E}{1-\nu^2} (\epsilon_p + \nu\epsilon_q)$$

$$\sigma_2 = \frac{E}{1-\nu^2} (\epsilon_q + \nu\epsilon_p)$$

$$\begin{aligned} \epsilon_p &= \frac{1247+902}{2} + \frac{1}{\sqrt{2}} \sqrt{(1247 + 1085)^2 + (1085 - 902)^2} \\ &= 2729 \end{aligned}$$

$$\begin{aligned} \epsilon_q &= \frac{1247+902}{2} - \frac{1}{\sqrt{2}} \sqrt{(1247 + 1085)^2 + (1085 - 902)^2} \\ &= -580 \end{aligned}$$

$$\begin{aligned} \sigma_1 &= \frac{210 \cdot 10^9}{1-0.3^2} (2728.541 + (0.3 \cdot (-579.541))) \\ &= 590 \text{ MPa} \end{aligned}$$

$$\begin{aligned} \sigma_2 &= \frac{210 \cdot 10^9}{1-0.3^2} (-579.541 + (0.3 \cdot 2728.541)) \\ &= 55 \text{ MPa} \end{aligned}$$

Vonmises stress is calculated from,

$$2\sigma_v^2 = (\sigma_1 - \sigma_2)^2 + (\sigma_2 - \sigma_3)^2 + (\sigma_3 - \sigma_1)^2$$

In this case $\sigma_3 = 0$

$$2\sigma_v^2 = (589.54118 - 55.158)^2 + (55.15 - 0)^2 + (0 - 589.54)^2$$

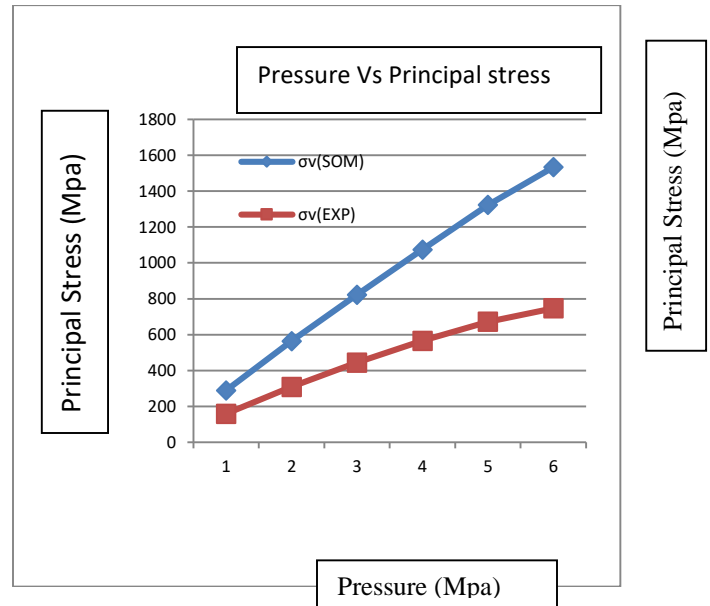
Therefore at location-1:

$$\sigma_v = 564 \text{ MPa}$$

Similarly principal stresses, principal strains and Vonmises stresses at other locations are calculated by above method and are tabulated as above table. Graphs are also plotted between

pressure being at X axis and principal stresses and Vonmises stress being at Y axis.

RESULTS: Pressure Vs Principal stress at location 1

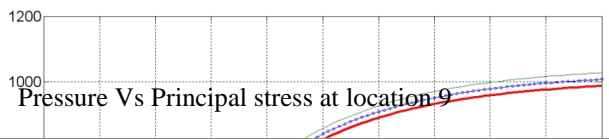
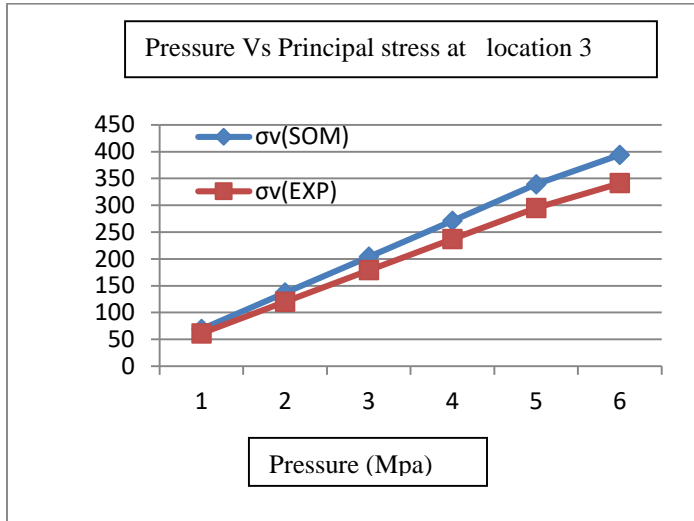


The experimental stresses at the location 1 are less than the calculated stresses from the strength of materials principles. And also all the experimental Vonmises stresses are not exceed the ultimate tensile strength of the 15CDV6. therefore this material is suitable for rocket motor casing at proposed thickness ($t=4.2\text{mm}$).

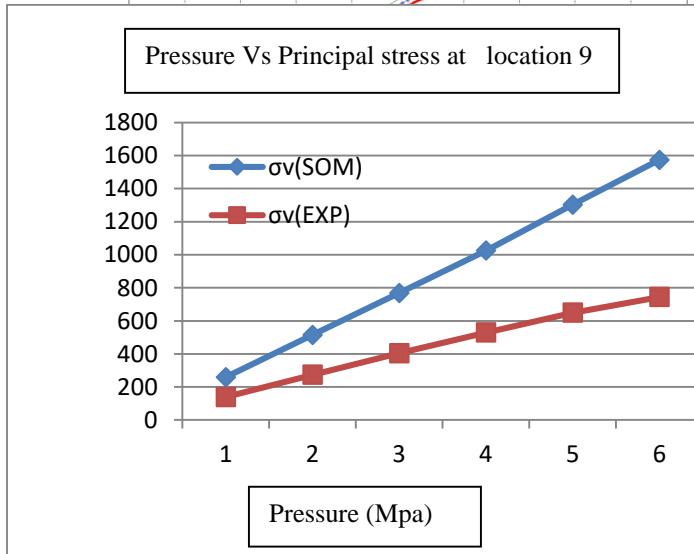
location	pressure(Mpa)					
	1		3		5.4	
	σ_{som}	σ_{exp}	σ_{som}	σ_{exp}	σ_{som}	σ_{exp}
1	290	160	823	445	1452	720
2	168	91	489	266	917	484
3	69	61	204	179	373	324
4	184	104	534	298	992	536
5	353	187	932	484	1791	808
6	114	59	477	246	968	489
7	111	64	448	250	2019	527
8	231	122	667	350	1249	622
9	259	139	768	404	1464	708



Pressure Vs Principal stress at location 3



Pressure Vs Principal stress at location 9



The experimental stresses at all the locations are less than the calculated stresses from the strength of materials principles. And also all the experimental Vonmises stresses are not exceed the ultimate tensile strength of the 15CDV6.therefore this material is suitable for rocket motor casing at proposed thickness(t=4.2mm).

VI CONCLUSION

Results and discussions:

1. Stresses/strains are increasing with increase in pressure.
2. The strain gauge at location-8 is bonded on the cylindrical region in the parent metal. The Stress calculated from classical theory and obtain from the test are compared.

$$\sigma = \frac{PD}{2t} = \frac{5.4 \times 1000}{2 \times 4.2} = 642 \text{ Mpa}$$

3. The stress from experiment is 633 MPa. This has a good agreement between calculation and experiment.
4. The stresses calculated by the Strength of material formula are higher, in some case more than the UTS of the material. The motor case has not failed in the test. This is because; the material 15CDV6 exhibits different non-linear stress strain behavior. A sample stress strain curve shown in below figure.

5. The stresses are recalculated by using the achieved stress strain curve and tabulated in the table 7.4 to 7.12.
6. These stresses should be compared with the tensile test coupon results and FOS should be arrived.
7. Vonmises stress at location-5 is slightly higher than yield strength. This is because of local low thickness observed at the particular location. This is because



of low thickness ($t < 4.2\text{mm}$) in the sheet itself due to bending.

8. The achieved material property is slightly higher than the specify yield strength that is 897MPa instead of 835MPa.

VII SCOPE OF FUTURE WORK

Carrying out pressure test on a solid rocket motor is costly and time consuming. The monitoring of health of motor strain gauges is local. Any failure initiation at a point where there are no strain gauges will not bring out the failure of the motor case. It is better to have health monitoring technique by use of acoustic emission which will give the overall health of the motor. It is better to have a database consisting of stress and strain values of more number of motor cases, that the motor can be accepted without doing the strain gauging and by using acoustic emission technique.

IX REFERENCES

- [1] Nacka, Richard Allan "Solid Propellant Rocket Motor Design and Testing", *April 1984, University of Manitoba*.
- [2] NASA SP-8025,"Solid rocket motor metal cases", *April 1970(N72-18785)*.
- [3] John D. Wrbanek and Gustave C. Fralick, "Thin Film Ceramic Strain Sensor Development for High Temperature Environments", *NASA/TM—2008-215256*.
- [4] Alain davenas, "Solid Rocket Propulsion Technology" *First English Edition 1993*.
- [5] R. Mischke& George, "*Rocket Propulsion Elements*" *7th Edition 2000*.
- [6] John D. Wrbanek, Gustave C. Fralick, and Gary W. Hunter, "Thin Film Ceramic Strain Sensor *Development for Harsh Environments*", *NASA/TM—2006-214466*
- [7] Joseph, shingly & Charles, "*Standard Handbook of Machine Design*" *3rd Edition*.